

OPTIMAL INFERENCE OF THE INVERSE GAMMA TEXTURE FOR A COMPOUND-GAUSSIAN CLUTTER

Patrick Fayard, Timothy R. Field

Department of Electrical and Computer Engineering
McMaster University, Hamilton, Canada

ABSTRACT

We first derive the stochastic dynamics of a Gaussian-compound model with an inverse Gamma distributed texture from Jakeman's random walk model with step number fluctuations. Following a similar approach existing for the K -distribution, we show how the scattering cross-section may be inferred from the fluctuations of the scattered field intensity. By discussing the sources of discrepancy arising during this process, we derive an analytical expression for the inference error based on its asymptotic behaviours, together with a condition to minimize it. Simulated data enables verification of our proposed technique. The interest of this strategy is discussed in the context of radar applications.

Index Terms— sea surface electromagnetic scattering, radar clutter, radar cross sections, stochastic differential equations, radar signal processing

1. INTRODUCTION

Compound-Gaussian models [1, 2] have been widely used to render the scattering amplitude retrieved from marine surfaces (especially with high-resolution radars). In effect, a random walk model with step number fluctuations [3] for the total scattered field yields such probability distributions for the scattered intensity where the (Gaussian) Rayleigh scattering is modulated by the variations in the scatterers population: the Radar Cross-Section (RCS). Besides the Gamma distribution, which results in a K -distributed scattered intensity, various other probability distributions may be chosen to model the RCS (e.g., an inverse Gamma distribution [4]). It was shown in [5], for an arbitrary cross-section, that one could extract this RCS from the (smoothing over a sample window of the) intensity-weighted fluctuations of the phase, a result relevant for radar processing applications to detect anomalies. However, due to the highly volatile phase variations, this inference process was heavily influenced by the smoothing process (i.e., over how many pulses the phase decoherence was averaged). In the K -distributed case, the error arising in this procedure was analytically studied and a condition, on the smoothing window length, was derived to minimize it as described in [6]. Whilst focusing on an *inverse* Gamma texture, which is

also of interest in radar applications, this paper aims to derive a corresponding analytical expression for the error arising during this inference process and optimize the smoothing (thus extending the strategy followed in [6]). The claims are illustrated by simulation data that compares this analytically tracked error with the discrepancy experimentally found.

2. RANDOM WALK MODEL

The scattered electric field is conveniently represented by a random walk model with a fluctuating number of steps N_t [3]

$$\varrho_t^{(N_t)} = \sum_{j=1}^{N_t} \exp(i\phi_t^{(j)}) \quad (1)$$

where the (independent) phasors $\{\phi_t^{(j)}\}$ are taken as a collection of Wiener processes $\phi_t = \Delta^{(j)} + \mathcal{B}^{1/2}W_t^{(j)}$, with the random initializations $\{\Delta^{(j)}\}$ a set of independent random variables uniformly distributed on the interval $[0, 2\pi)$. The *rationale* is understood as follows: within the illumination range of a radar will be present a time-varying population of scatterers, assumed to behave identically. The scattered amplitude results as the summation of the scatterers' individual contributions.

Using Ito's formula for (1) enables to write the following Stochastic Differential Equation (SDE) for the (normalized) process $\gamma_t = \lim_{N \rightarrow \infty} [\varrho_t^{(N_t)} / N_t^{1/2}]$ for a constant population,

$$d\gamma_t = -\frac{1}{2}\mathcal{B}\gamma_t dt + \mathcal{B}^{1/2}d\xi_t \quad (2)$$

in terms of the complex Wiener process ξ_t (which satisfies $|d\xi_t|^2 = dt$ and $d\xi_t^2 = 0$). γ_t is therefore a complex Ornstein-Uhlenbeck process, labeled speckle in radar processing applications. The inverse of the constant \mathcal{B} , characterized by the carrier wavelength according to $\mathcal{B} \sim c|k|$, is a characteristic time for the autocorrelation of γ_t .

If the number of scatterers fluctuates with time, we introduce the scattering amplitude ψ_t , normalized by the population mean \bar{N} , for which the following compound representa-

tion holds:

$$\begin{aligned}\psi_t &= \lim_{N_t \rightarrow \infty} \left[\varrho_t^{(N_t)} / \bar{N}^{1/2} \right] \\ &= \lim_{N_t \rightarrow \infty} \left[(N_t / \bar{N})^{1/2} (\varrho_t^{(N_t)} / N_t^{1/2}) \right] \\ &= x_t^{1/2} \gamma_t\end{aligned}\quad (3)$$

where $x_t = \lim_{N_t \rightarrow \infty} [N_t / \bar{N}]^{1/2}$ is the scattering cross-section (i.e., the texture). Equation (3) represents the scattered amplitude as the product of two processes inherently independent: the population evolution x_t and the Rayleigh amplitude scattered from a constant number of scatterers.

3. CHOICE OF THE TEXTURE

The discussion above pertains to any compound-Gaussian model, which is characterized by selecting a probability distribution for the RCS x_t . The primary criterion to support such a choice is the closeness to experimental scattering data. A widely accepted model, the K -distribution, posits a Gamma distribution for the RCS [3]. We shall here consider an alternative inverse Gamma distribution for the texture x

$$\mathcal{P}_\infty = \frac{x^{-(\alpha+1)} \exp^{-1/x}}{\Gamma(\alpha)} \quad (4)$$

which has also been justified on experimental grounds in [4]. In other words, the random variable $u = 1/x$ is Gamma distributed. The first two moments of the distribution (4) read $\langle x \rangle = (\alpha - 1)^{-1}$ and $\text{Var}[x] = (\alpha - 1)^{-2} (\alpha - 2)^{-1}$ and exist for $\alpha > 1$ and $\alpha > 2$ respectively.

This distribution can be seen as the asymptotic distribution of a probability density that obeys the following Fokker-Planck equation on a suitable timescale:

$$\frac{1}{\mathcal{A}} \frac{\partial \mathcal{P}}{\partial t} = -\frac{\partial[\beta \mathcal{P}]}{\partial x} + \frac{\partial^2[\sigma^2 \mathcal{P}]}{\partial x^2} \quad (5)$$

where β and σ^2 represent, respectively, the drift and volatility coefficients. The autocorrelation characteristic time of the RCS \mathcal{A}^{-1} is (experimentally) much greater than \mathcal{B}^{-1} (of the order of many seconds and milliseconds, respectively [6]). In other words, the rapidly varying speckle is modulated by a long timescale RCS. It may be verified that the probability distribution (4), with parameters $\beta = 1 - (\alpha - 1)x$ and $\sigma = x$, is indeed the asymptotic distribution for (5)¹.

An alternative representation of the FPE (5), which facilitates subsequent derivations of the scattered amplitude dynamics, is the following SDE,

$$dx_t = \mathcal{A}(\alpha - 1)(\alpha - x_t)dt + (2\mathcal{A}x_t^2)^{1/2} dW_t^{(x)}, \quad (6)$$

in terms of the rescaled process: $x_t \rightarrow \alpha(\alpha - 1)x_t$. As the local Rayleigh power, x_t should remain positive. Consistently

¹note that the asymptotic distribution does not determine uniquely the drift and volatility parameters

we observe from (6) that there exists a natural boundary at $x_t = 0$ (provided $\alpha > 1$, i.e., that the first moment of the RCS exists) since the volatility vanishes and the drift is positive there. Echoing the similar property existing for a Gamma distribution, (6) also guarantees an exponential decay in the autocorrelation function (for $\alpha > 1/2$) [7].

4. DYNAMICS OF THE SCATTERING AMPLITUDE

The dynamics of the intensity $z_t = |\psi_t|^2$ and phase $\theta_t = \angle(\psi_t)$ can be obtained from (2) and (6) [5]. In effect, the intensity dynamics obey the equation

$$\begin{aligned}dz_t &= \left[\mathcal{A} \left(\frac{(\alpha - 1)(\alpha - x_t)z_t}{x_t} \right) + \mathcal{B}(x_t - z_t) \right] dt \\ &\quad + (2\mathcal{A}z_t^2)^{1/2} dW_t^{(x)} + (2\mathcal{B}x_t z_t)^{1/2} dW_t^{(r)}\end{aligned}\quad (7)$$

where

$$(\gamma_t^* d\xi_t + \gamma_t d\xi_t^*) = \left(\frac{2z_t}{x_t} \right)^{1/2} dW_t^{(r)}. \quad (8)$$

Similarly, the phase is governed by the SDE

$$d\theta_t = \left(\frac{\mathcal{B}x_t}{2z_t} \right)^{1/2} dW_t^{(\theta)} \quad (9)$$

where

$$\frac{1}{i}(\gamma_t^* d\xi_t - \gamma_t d\xi_t^*) = \left(\frac{2z_t}{x_t} \right)^{1/2} dW_t^{(\theta)}. \quad (10)$$

We note that the two Wiener processes arising above, $dW_t^{(r)}$ and $dW_t^{(\theta)}$, are independent (the radial and angular fluctuations in the resultant amplitude are statistically independent).

Although the K -distributed disturbance is often discussed in the literature, this exposition in terms of a set of SDEs is less common. Its main advantage is as follows. Instead of considering the mere moments of the scattered intensity, the coupled system (6) and (7) captures the dynamics permitting, for instance, to derive analytically the autocorrelation function of z_t or any higher-order temporal statistic. Another significant advantage is the possibility of generating K -distributed samples through a finite difference scheme.

5. CROSS-SECTION INFERENCE

At this point, we shall recall a proposition from [5] which states that the instantaneous values of the scattering cross-section are observable through the intensity-weighted squared phase fluctuations, as shown by:

$$x_t = \frac{2}{\mathcal{B}} z_t d\theta_t^2 / dt. \quad (11)$$

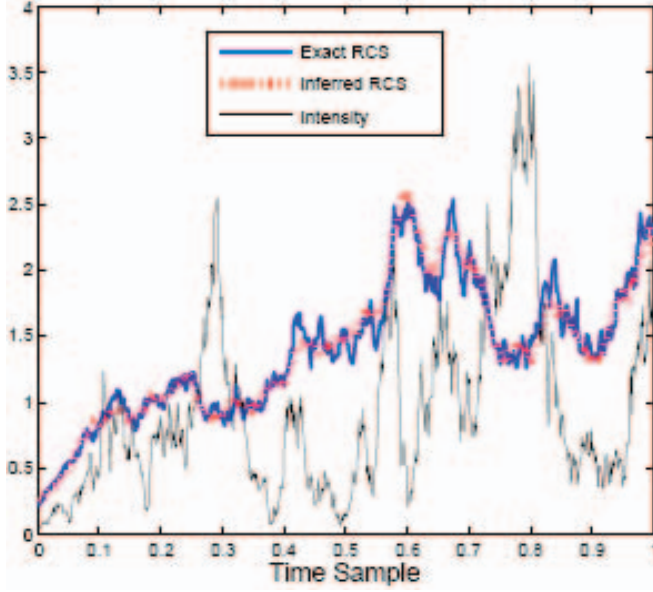


Fig. 1. Inference of the scattering cross-section/population through the effect of phase decoherence. (For parameter values $\alpha = 4$, $\mathcal{A} = 10^{-4}$, $\mathcal{B} = 10^{-3}$.)

The efficiency this proposition is verified for synthetically generated data by adapting the simulation performed in the case of K -scattering [5] for our inverse Gamma texture (i.e., the drifts and volatility parameters corresponding to the K -scattering case, $\beta = (\alpha - x)$ and $\sigma^2 = x$, are respectively substituted by $\beta = 1 - (1 - \alpha)x$ and $\sigma^2 = x^2$). An Ito finite difference scheme enables to generate samples of the scattered amplitude, through (3), as the result of the (independent) integrations of the complex Gaussian process (2) and of the population dynamics (6).

The results of the simulation are provided in Figure 1 which shows time series for the scattered intensity (observed state), the exact cross-section generated in the simulation (unknown state) and the values of the state inferred from the phase fluctuations. The estimate of the state follows from (11) which implies, for discretely sampled data,

$$z_i \delta \theta_i^2 \propto x_i n_i^2 \quad (12)$$

where $\{n_i\}$ are an independent collection of $\mathcal{N}(0, 1)$ distributed random variables.

Applying a smoothing average $\langle \cdot \rangle_\Delta$ to the left-hand side (the observations) of (12) with window $\Delta = [t_0 - \Delta\delta_t, t_0 + \Delta\delta_t]$ yields an approximation to x_{t_0} . An alternative expression for (12) makes use of the independence between n_t and x_t (as evidenced by (3) and (10)).

$$\langle x_i \rangle_\Delta \propto \frac{\langle z_i d\theta_i^2 \rangle_\Delta}{\langle n_i^2 \rangle_\Delta} \quad (13)$$

6. OPTIMIZATION OF THE INFERENCE

Equation (13) reveals the two distinct phenomena that will yield a discrepancy between the exact state and its smoothed value inferred from the intensity fluctuations. If the number of samples contained within the smoothing window is too small, the variance of $\langle n_i^2 \rangle_\Delta$ will be high. *A contrario*, if the window length is too large, the instantaneous fluctuations of the RCS are not captured well enough since the average $\langle z_i d\theta_i^2 \rangle_\Delta$ produces a loss of information. Since these two effects vanish for, respectively, large and small Δ , we may assert that the total error may be written as the summation of these two asymptotic behaviours. The error for the first case, ϵ_{n_i} , when Δ is small reads as follows since $\langle x_i \rangle_\Delta \approx x_i$

$$\epsilon_{n_i} = \sum_{i=1}^N \mathbf{E} \left[(\langle n_i^2 \rangle_\Delta x_i - x_i)^2 \right] \quad (14)$$

$$= \sum_{i=1}^N \mathbf{E} [x_i^2] \mathbf{E} [(\langle n_i^2 \rangle_\Delta - 1)^2] \quad (15)$$

$$= \frac{2}{\Delta} \left(\sum_{i=1}^N \mathbf{E} [x_i^2] \right). \quad (16)$$

where we have used $n_i^2 \sim \chi^2(1)$ and $\text{Var}[n_i^2] = 2$. The situation of the error for a large window length, ϵ_{x_i} , is somehow more complex. Here, the deviation may be written

$$\epsilon_{x_i} = \sum_{i=1}^N \mathbf{E} [(\langle x_i \rangle_\Delta - x_i)^2] \quad (17)$$

since $\langle n_i \rangle_\Delta \approx 1$. If we consider the discrete version of (6),

$$x_{i+1} = (1 - (\alpha - 1)\mathcal{A}\delta_t) x_i + \alpha(\alpha - 1)\mathcal{A}\delta_t + (2\mathcal{A}\delta_t x_i^2)^{1/2} w_i \quad (18)$$

where $w_i \sim \mathcal{N}(0, 1)$. Since $\mathcal{A}\delta_t \ll 1$, $1 - (\alpha - 1)\mathcal{A}\delta_t \approx 1$ (the fluctuations of the RCS being negligible within the sampling window); yielding the iterated expression

$$x_{i+j} = x_i + j\alpha(\alpha - 1)\mathcal{A}\delta_t + \sum_{k=1}^{|j|} (2\mathcal{A}\delta_t)^{1/2} x_{i+\text{sg}(j)k} w_{i+\text{sg}(j)k} \quad (19)$$

The inner term in (17) therefore reads

$$\langle x_i \rangle_\Delta - x_i = \frac{1}{\Delta} \sum_{j=-\frac{\Delta}{2}}^{\frac{\Delta}{2}} \left[j\alpha(\alpha - 1)\mathcal{A}\delta_t + \sum_{k=1}^{|j|} (2\mathcal{A}\delta_t)^{1/2} x_{i+\text{sg}(j)k} w_{i+\text{sg}(j)k} \right] \quad (20)$$

where $j\alpha(\alpha - 1)\mathcal{A}\delta_t$ vanishes, since it is odd. A subsequent derivation, using $\mathbf{E}[w_i w_j] = \delta_{i-j}$, yields

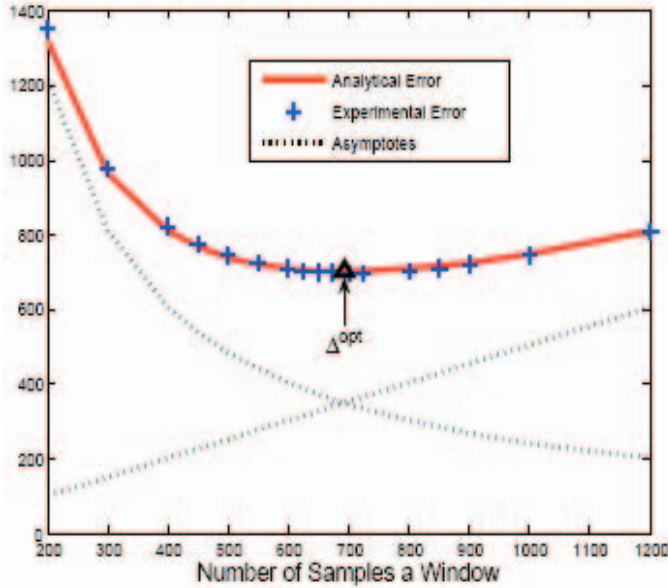


Fig. 2. Comparison of the experimental and analytical MSE deviations between the inferred and the exact cross-sections.

$$\epsilon_{x_i} = \frac{\mathcal{A}\delta_t\Delta}{6} \left(\sum_{i=1}^N \mathbf{E} [x_i^2] \right). \quad (21)$$

for the asymptotic error (cf. [6] for details). Armed with analytical expressions for its asymptotes, (16) and (21), the total smoothing error may be written

$$\epsilon = \left[\frac{\mathcal{A}\delta_t\Delta}{6} + \frac{2}{\Delta} \right] \left(\sum_{i=1}^N \mathbf{E} [x_i^2] \right), \quad (22)$$

out of which we readily derive the following condition on the smoothing window length for the inference to be optimized

$$\Delta^{\text{opt}} = \left(\frac{12}{\mathcal{A}\delta_t} \right)^{1/2} \quad (23)$$

For our inverse Gamma texture, the validity of (22) is established by computing the MSE deviation between the inferred and the exact cross-sections over a range of window length Δ . Figure 2 (where the parameter values are the same as for Figure 1) shows that the analytical error (solid line) captures accurately the experimental error (markers).

7. CONCLUSION

Following a strategy exposed in [5] we have discussed how, for an arbitrary diffusion model for the texture, exemplified herein by an inverse Gamma distribution, it is possible to infer the RCS from the fluctuations of the scattered intensity

and phase. Next, we have derived an analytical expression for the error resulting from this inference process and we have provided a condition, on the number of pulses over which the phase decoherence must be averaged, to minimize it. Thus, the procedure described in [5] has been improved. The procedure developed in this paper may readily be extended to various other diffusion models for the texture and future work should focus on the corresponding situations for existing recognized Gaussian-compound clutters. The Pearson class of diffusion processes [8] is of particular interest since, on account of the corresponding linear drift in (6), it will proceed along the same steps (except for the substitution of the *ad hoc* volatility parameter in (21)). These results are firstly expected to improve the procedure detailed in [5] to observe the RCS and secondly to extend it to other compound Gaussian-distributions. In addition, they may also be relevant for other fields where compound Gaussian-models are commonly used (e.g., radio propagation channel disturbances).

8. REFERENCES

- [1] A. Farina, F. Gini, M.V. Greco, and L. Verrazzani, "High resolution sea clutter data: statistical analysis of recorded live data," *IEE Proc. Radar, Sonar and Navigation*, vol. 18, no. 3, pp. 121–130, Jun 1997.
- [2] F. Gini, M.V. Greco, M. Diani, and L. Verrazzani, "Performance analysis of two adaptive radar detectors against non-Gaussian real sea clutter data," *IEEE Trans. Aerosp. Electron. Syst.*, vol. 36, no. 4, pp. 1429–1439, Oct 2000.
- [3] E. Jakeman and R.J.A. Tough, "Non-Gaussian models for the statistics of scattered waves," *Adv. Phys.*, vol. 37, pp. 471–529, 1988.
- [4] A. Balleri, A. Nehorai, and J. Wang, "Maximum likelihood estimation for compound-Gaussian clutter with inverse Gamma texture," *IEEE Trans. Aerosp. Electron. Syst.*, vol. 43(2), pp. 775–780, Apr 2007.
- [5] T.R. Field, "Observability of the scattering cross-section through phase decoherence," *J. Math. Phys.*, vol. 46(6), pp. 063305 1–8, Jun 2005.
- [6] P. Fayard and T.R. Field, "Optimal inference of the scattering cross-section through the phase decoherence," *Waves Random Complex Media*, vol. 18(4), pp. 571–578, Nov 2008.
- [7] E. Wong, "Construction of a class of stationary Markoff processes," in *XVIth Symp. Appl. Math.* Amer. Math. Soc. Proc., 1963, vol. II, pp. 264–276.
- [8] Y. Delignon and W. Pieczynski, "Modelling non-Rayleigh speckle distribution in SAR images," *IEEE Trans. Geosci. Remote Sens.*, vol. 40(6), pp. 1430–1435, Jun 2002.